What can Superconducting Gravimeters contribute to normal mode seismology?

R. Widmer-Schnidrig

Black Forest Observatory, Heubach 206, D-77709 Wolfach, Germany
e-mail: widmer@geophys.uni-stuttgart.de

1. Introduction

Superconducting gravimeters (SGs) currently deployed in the sparse GGP network [*Crossley et al.*, 1999] hold the promise to achieve lower instrumental noise levels over sensors currently deployed in the Global Seismographic Network (GSN) and used in studies of the Earth's free oscillations.

This position paper attempts to review the current situation in observational normal mode seismology: both from the point of view of instrumental challenges and challenges related to the illumination of the Earth's large-scale structure.

Particular attention is given to 1-D and 3-D density structure and how this structure is encoded in the observable normal mode spectra. The reason for concentration on density structure is that the frequency band where SGs compare most favorably with seismic sensors coincides with the band where the modes have increased sensitivity to laterally heterogeneous as well as 1-D density structure through the mechanism of self-gravitation. Since our ability to learn about Earth structure is always a question of signal-to-noise ratio (SNR) in our data we have organized the paper into a discussion of instrumental and environmental noise followed by a discussion of normal mode signals.

The paper concludes with an assessment of where SGs can make a difference in our quest to learn about deep Earth structure.

2. Vertical Seismic Noise

2.1. Global Noise Models

The level of background seismic noise limits our ability to detect small seismic signals which have propagated through the Earth and which carry information about both their source and the structure of the medium through which they propagated. Comprehensive studies of typical and of minimum noise levels have been carried out to asses station performance, to help in site selection, and in negotiations of nuclear test ban treaties [e.g. *Agnew and Berger*, 1978; *Peterson*, 1993; *Astiz and Creager*, 1995]. Figure 1 shows the new Low Noise Model of *Peterson* [1993] which is the lower envelope of noise levels found at GSN stations. A number of different sensors are deployed at the GSN stations, however, below 30 mHz the NLNM is largely defined by the Streckeisen STS-1 seismometer.

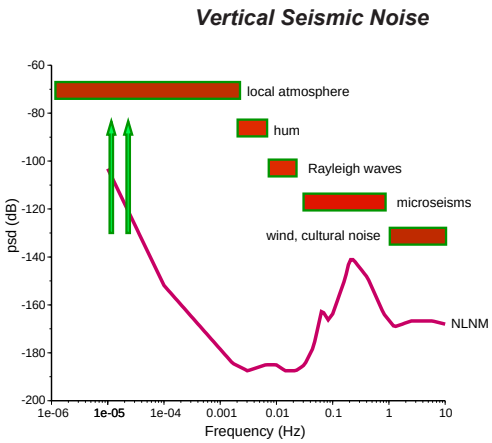

Figure 1. Dominant sources of seismic noise on vertical component sensors (*i.e.* gravimeters and vertical seismometers) together with the New Low Noise Model (NLNM) of *Peterson* [1993]. The NLNM is the lower envelope of noise spectra at GSN sites and represents the least expected noise level for seismic observatories. The NLNM is given in power spectral densities in units of dB relative to 1 $(m/s^2)^2/Hz$.

Many of the large features of the NLNM are well understood. At frequencies below 2 mHz the Newtonian attraction of moving air masses in the local atmosphere above the seismic sensor is the principal source of noise [e.g. *Warburton and Goodkind*, 1977; *Zürn and Widmer*, 1995].

In the band 2-7 mHz the NLNM exhibits a slight minimum near 3 mHz but is otherwise relatively flat. Recent studies of the noise floor in this band with high frequency resolution have revealed that the noise floor contains a well defined structure consisting of ∼50 regularly spaced peaks whose frequencies coincide with the fundamental spheroidal modes, ${}_0S_\ell$ [e.g. *Suda et al.*, 1998]. This structure in the noise floor is termed background free oscillations or simply *hum*. Since free oscillations are a global phenomenon the hum constitutes a lower bound for observable signals at any site on the Earth's surface. The hum amplitude has also been found to be very stable in time with only a small semi-annual harmonic component. In the band 7 - 30 mHz the NLNM exhibits a local maximum near 10 mHz.

The cause for the generally level noise floor between 2 and 30 mHz is still not understood. However *Nishida et al.* [2002, manuscript in preparation] were able to demonstrate that in the band adjacent to the hum (7-30 mHz) the background noise consists of globe circling Rayleigh waves much like the hum [*Ekström*, 2001]. The physical process involved in the hum excitation is still a matter of debate with turbulence in the atmosphere and/or hydrosphere being the favored candidates.

One problem with identifying the source is the small size of the signal: to drive one of the spheroidal multiplets at the observed *rms* amplitudes (∼ 1 ngal or 5×10^{-10} m/s at 300 seconds period, a quality factor of the mode of $Q \sim 300$ and an effective mass of the upper mantle of $m \sim 10^{24}$ kg) requires approximately 10 Watts of power! Another more serious problem is that the hum signal is very close to the detection limit of current sensors (see below).

In the band 30 mHz - 1 Hz background noise levels are dominated by the marine microseism with a peak around 0.14 Hz. The cause of the microseism are the swell- and surf-induced pressure fluctuations at the bottom of the water column which excite seismic waves in the solid Earth. It is very fortunate for the study of normal modes that the normal mode band (0.3 - 20 mHz, fig. 6) and the band of microseism (30 mHz - 1 Hz) do not overlap considering that noise levels in the microseism band are often 60 dB higher than in the band of the hum.

2.2. Noise levels at BFO

The Black Forest Observatory is particularly suited for noise studies because of two reasons: (1) noise levels at BFO have been repeatedly shown to be among the

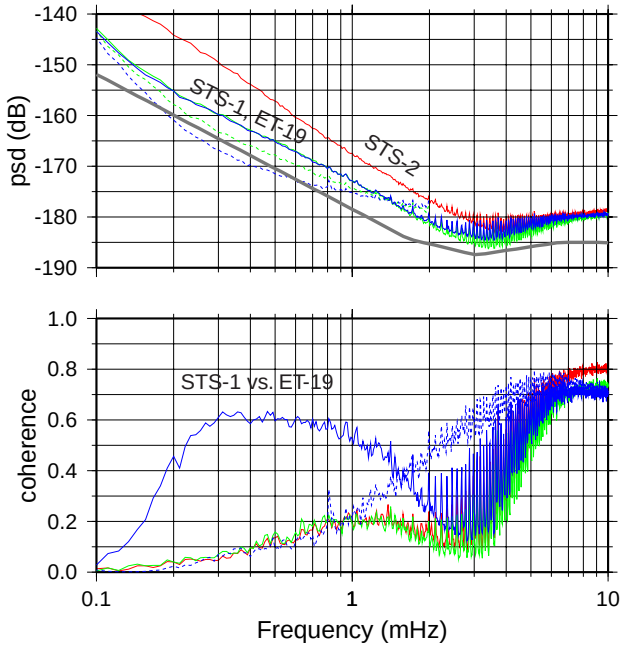

Figure 2. Comparison of the three vertical component seismic sensors installed at BFO: LaCoste-Romberg gravimeter ET-19 and Streckeisen STS-1 and STS-2 seismometers. Shown are the noise levels averaged over the 895 selected windows. The dashed curves are the pressure corrected STS-1 and ET-19 noise levels [*Zürn and Widmer*, 1995]. For the STS-2 the pressure correction is ineffective. The NLNM is shown for reference.
The lower panel shows average pairwise coherencies: STS-2 vs. STS-1 (red), STS-2 vs. ET-19 (green) and STS-1 vs. ET-19 (blue). The coherencies between the STS-2 and either STS-1 or ET-19 is low below ∼5 mHz due to the increased noise levels in the STS-2. In the Band 2-4 mHz the coherency between STS-1 and ET-19 is also very low which shows that in this band the self-noise levels of these two sensors are comparable to the level of the (coherent) signal.
The dashed curve in the lower panel is the coherency between the pressure corrected spectra of ET-19 and STS-1. Its low value for frequencies less than 1 mHz shows that at least one of the sensors (the STS-1) is limited by self-noise after the pressure correction. Since the pressure correction is marginally efficient for the STS-1 and since uncorrected noise levels of STS-1 and ET-19 are practically identical, we conclude that the NLNM in this band is defined by the barometric effect. The increase of the pressure corrected coherency above 1 mHz is an artefact of the pressure correction, which only reduces noise levels below 1.5 mHz. Finally, we note the small peak in the pressure corrected coherency at 0.81 mHz - the frequency of ${}_0S_0$.

lowest of the GSN [e.g. *Zürn et al.*, 2000] and (2) these low noise levels have been achieved simultaneously with up to four different sensors [*Richter et al.*, 1995].

Thus one can attempt to answer the question to what extent the NLNM is defined by the instrumental noise of the sensors or by seismic noise. While this distinction is impossible to make with a single sensor, it is also dangerous to conclude from global studies such as the one by *Peterson* [1993] that the universality of the NLNM is a feature of the Earth's seismic background. Considering that the NLNM below 20 mHz relies primarily on data from STS-1 seismometers it is conceivable that the NLNM reflects (at least in some bands) the instrumental noise of the STS-1.

With multiple co-located sensors it is possible to separate sensor noise from seismic noise. Seismic noise should be common to all sensors while sensor noise should be uncorrelated between the different sensors.

To get a robust and representative estimate of seismic noise at BFO we have selected data from the vertical component STS-1 seismometer (VHZ) recorded on a 24 bit channel of the IDA Mk7 data logger, the TIDE channel of the LaCoste-Romberg ET-19 gravimeter (UGZ) recorded on a 16 bit auxiliary channel of the IDA Mk7 logger and the long-period channel (LHZ) of the STS-2 seismometer of the German Regional Seismic Network (GRSN) recorded with 24 bits on a Quanterra Q680 data logger. Continuous data for a 3 year window (1996:206 - 1999:179) was chopped into 24 hour long, overlapping segments with start times at midnight and at noon. Segments were only retained if data from all three sensors was complete. Power spectral densities were computed and integrated between 3 - 5 mHz to give a single number representative of noise level in the normal mode band. Based on a histogram of these noise levels a selection of 895 quiet windows was made for which all three sensors simultaneously meet our noise criterion. Thus 60 % of the windows were rejected.

Fig. 2 (top) shows the average power spectral densities for the three sensors. At frequencies below 2 mHz the psd of the STS-1 and the ET-19 sensors are very similar. This is probably because both instruments are sensitive enough to record the gravity signal from the moving air masses in the atmosphere above the station. If we apply the barometric correction [*Zürn and Widmer*, 1995], however, psd levels drop by different amounts. Histograms of regression coefficients for the three sensors are given in fig. 4. At 0.3 mHz the pressure correction reduces psd levels by $\sim$ 2 dB for the STS-1 but by as much as 7 dB for ET-19. Thus it becomes clear that self noise of the STS-1 in this band is only slightly below the signal psd whereas for ET-19 it is well below the signal level.

The low efficiency of the pressure correction for the STS-1 cold be due to a noisy integral feedback. To check this hypothesis the electronics of the STS-1 at BFO was

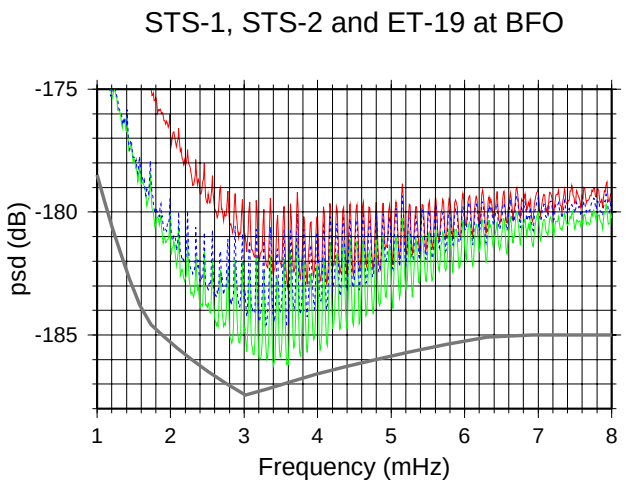

Figure 3. Blow-up of upper panel of fig 2. The lowest curve (green) is from the STS-1, followed by the ET-19 (blue, dashed) and the STS-2 (red).

modified but this modification did not lead to any improvement [*Wielandt and Zürn, pers. comm., 1999*].

The pairwise coherencies are given in the lower panel of fig. 2. In the band of the hum the STS-1 seems to be the sensor with the lowest self noise followed by the ET-19 and STS-2.

Fig. 3 zooms in on the hum part of fig 2. The comb like structure of the spectra is typical for the hum. Note the slight increase of the hum near 3.7 mHz. This amplification of the hum was noted by *Nishida et al.* [2000] and constitutes the most direct observational evidence for atmospheric excitation of the hum. Note that at 4 mHz the STS-2 is only 3 dB noisier than the STS-1 while this difference increases to 10 dB at the frequency of ${}_0S_2$ or 0.3 mHz.

2.3. Noise levels of SG meters

Since we do not operate a permanently installed SG meter at BFO we refer to published comparisons of SG meter noise levels and our permanent sensors: *Richter et al.* [1995] have compared data from the seismometers and the LaCoste-Romberg gravimeter with a temporarily installed, portable SG meter (SG102), while *Banka and Crossley* [1999] and more recently *Van Camp* [1999] compare SG meters contributing to the GGP network with our sensors.

For frequencies above 1.5 mHz these studies find that the STS-1 and ET-19 at BFO are less noisy than the SG meters. This finding has also been confirmed in studies of the hum at Canberra (Australia) where an STS-1 and an SG are co-located [*Nawa et al.*, 2000]. In the hum band average noise levels for the STS-1 are $\sim$7 dB lower than for the best SG meters while ET-19 is only 4 dB lower. (These numbers were obtained by converting the noise-magnitude estimates of [*Van Camp*, 1999] into

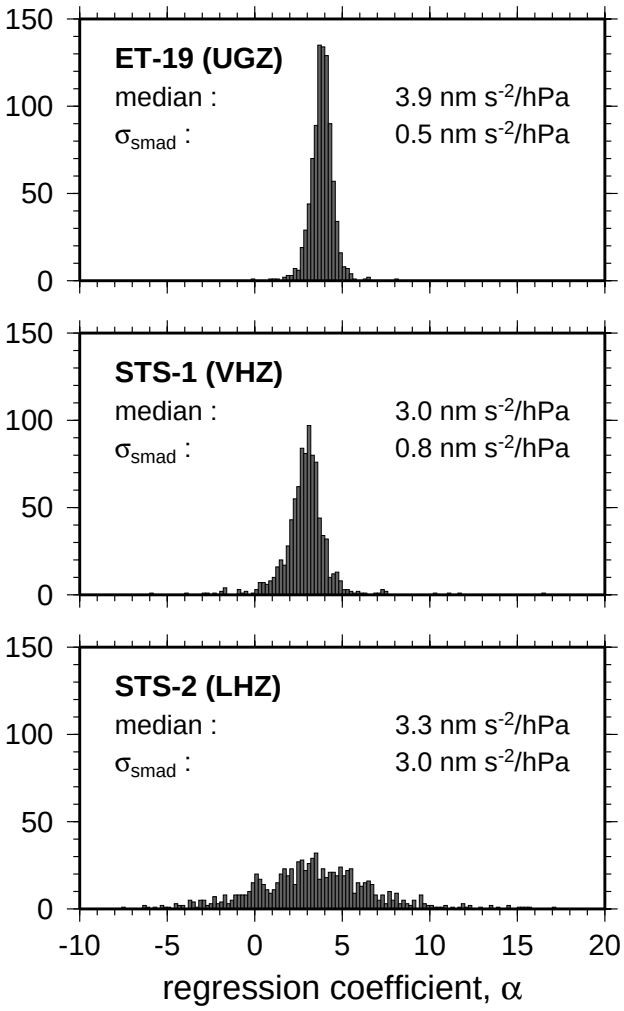

Figure 4. Histograms of 895 regression coefficients for the pressure correction. The regression was carried out in the band 0.1 - 0.5 mHz. Note the large dispersion for the STS-2. σ_{SMAD} is the scaled median absolute deviation of the median - a statisticaly robust measure of dispersion equivalent to the standard deviation.

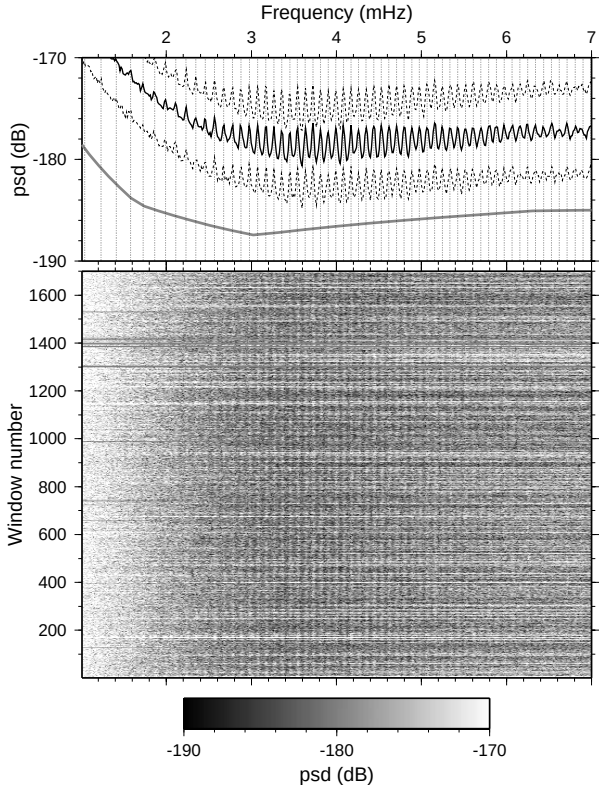

Figure 5. Time-frequency plot covering 2 years of data from the STS-2 seismometer of the German Regional Seismic Network (GRSN) at BFO. The range of the gray scale is chosen to emphasize structure in the noise during seismicaly quiet times. The upper panel shows median psd levels (black) together with the first and third quartile (dashed). The NLNM (gray) is shown for reference. The vertical dashed lines indicate the predicted frequencies of the fundamental spheroidal modes ${}_0S_\ell$ and coincide with light-grey bands in the lower panel.

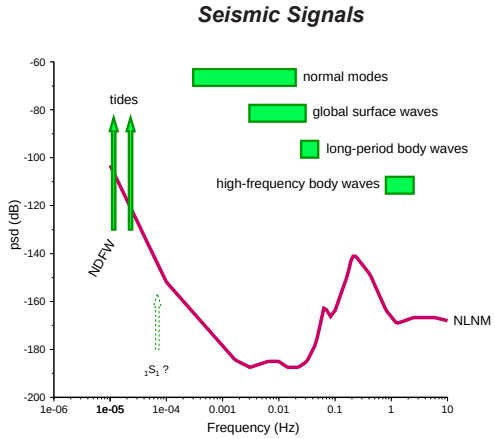

Figure 6. Principal signals in vertical seismic recordings. The suspected location of the Slichter mode, $_1S_1$ is also indicated.

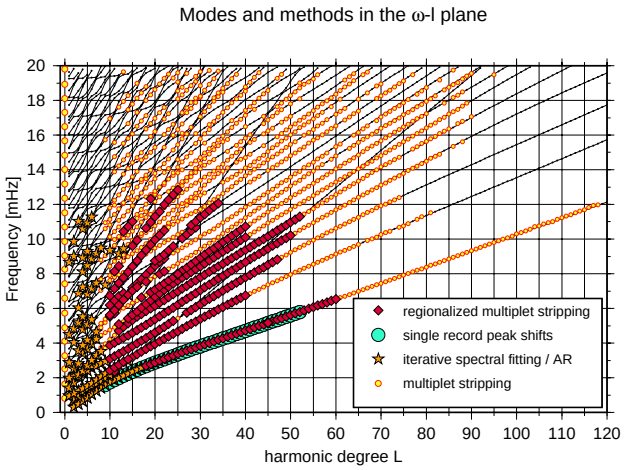

Figure 7. Spheroidal mode dispersion diagram for model PREM. The symbols used for the different modes indicates the analysis technique with which the mode was observed: regionalized multiplet stripping [*Widmer-Schnidrig*, 2002], single record peak shifts [e.g. *Smith and Masters*, 1989], iterative spectral fitting [e.g. *Ritzwoller et al.*, 1988], autoregressive method (AR) [*Masters et al.*, 2000], multiplet stripping [*Masters and Widmer*, 1995].

equivalent psd values). This difference in noise levels is also consistent with the observation that the psd levels of the best SGs intersect - after pressure correction - the NLNM at a frequency of ∼1 mHz.

For frequencies below 1.5 mHz where the barometric pressure correction is efficient for gravimeters, the best SGs are less noisy than STS-1 seismometer. While SGs could still not compete with the ET-19 gravimeter in this band back in 1994 [*Richter et al.*, 1995], recent improvements in the SG meters has changed this picture. [*Zürn et al.*, 2000]. In this article data from the Balleny Islands event (1998) recorded by IRIS, GEOSCOPE and GGP networks was systematically scanned for signals of Coriolis coupled modes below 1 mHz and the highest SNR was found in the spectra of SG meters and ET-19. The most recent occasion for the observation of the gravest normal modes was the Peru event with moment magnitude M_W=8.3 on June, 23 2001 and the spectrum of the SG near Strasbourg (J9) is shown together with the spectrum of the 1977 Sumbawa event (M_W=8.3) recorded in Brasilia with the IDA gravimeter at Brasilia (BDF) in fig. 9. The spectrum from BDF was up until now the spectrum with the highest signal-to-noise ratio for the football mode, $_0S_2$. For the Peru event this mode was detected with similar SNR in spectra of SG meters located in Vienna (Austria), Metsähovi (Finland), Moxa (Germany), and Southerland (South Africa) and their heigh SNR for $_0S_2$ could not be matched with either ET-19 or any of the STS-1s of the GSN.

In other words the most recent version of SGs are now competitive with the best spring gravimeters as far up in frequency as 1.5 mHz and below ∼0.6 mHz they are – after pressure correction – clearly superior to either spring gravimeters or STS-1 seismometers..

Above 3 mHz, however, it seems that the best SGs cannot compete with the STS-2 at BFO. To corroborate the low noise level of the STS-2 at BFO we show a spectrogram of 2 years of continuous data (fig. 5) together with a robust estimate of the noise levels of that sensor. While one might suspect that this low noise level of the STS-2 is due to the very elaborate shielding of the sensors at BFO, it should be noted that we detected the hum at 7 out of 14 STS-2 equipped stations of the German Regional Seismic Network (GRSN).

The low noise level of the STS-2 above 3 mHz, while higher than STS-1 or ET-19 is of some practical relevance since manufacturing of both LaCoste-Romberg ET meters as well as STS-1 seismometers has been discontinued, making the STS-2 the quietest, commercially available sensor in this band. (Note: we have not inspected data from Geotech KS-54000 borehole seismometer which are also deployed in the GSN for hum signals and are also unaware of any published hum detections for that sensor. The same is true for broad-band seismometers manufactured by Guralp).

3. Normal modes in seismic data

Before the Earth's normal modes can be detected as discrete peaks in spectra of earthquake recordings a number of criteria must be met: The earthquake source must exceed a minimum moment magnitude of M_w ∼6.5.

Since the modes can be viewed as the interference of waves traveling in opposite direction around the globe,

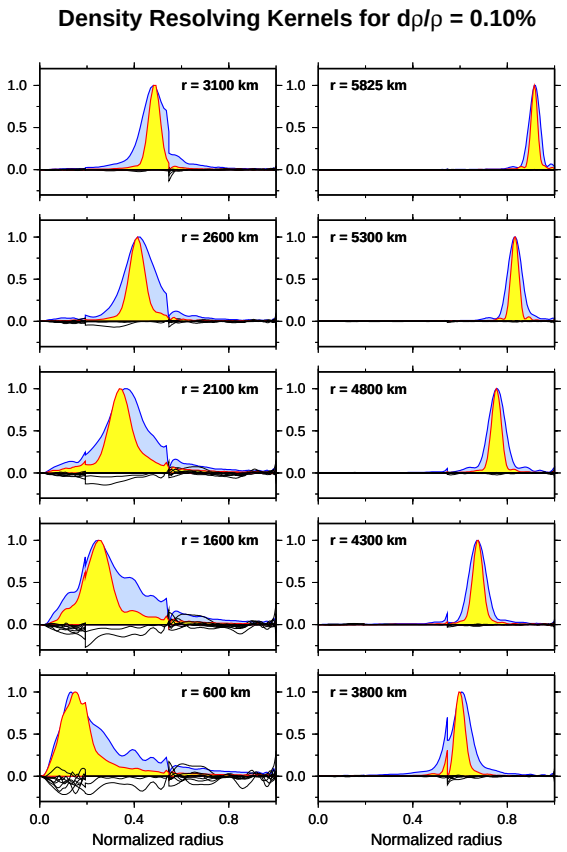

Figure 8. Backus-Gilbert type resolution analysis for the radial distribution of density. The narrower (yellow) averaging kernels include the new degenerate frequency estimates made possible by the sequence of large events in 1994. The wider (blue) averaging kernels are solely based on the degenerate frequency dataset compiled in *Masters and Widmer* [1995] which was derived from earthquake recordings prior to 1994. The width of the bell-shaped curve is a measure of the ability of the data to concentrate information regarding a particular parameter (here density) and a given variance (0.1 percent). The data of the events in 1994 have significantly improved our ability to resolve 1-D density structure.

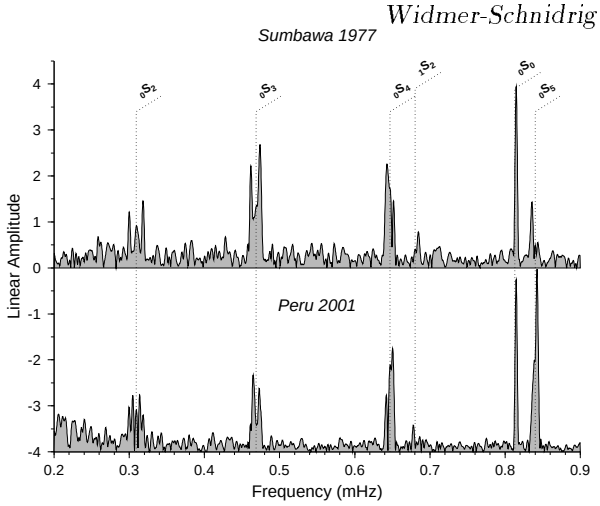

Figure 9. Comparison of two spectra from events separated by 24 years. The upper spectrum is for the 1977 Mw8.3 Sumbawa event recorded with the LaCoste-Romberg gravimeter at BDF and the lower spectrum is for the 2001 Mw8.4 Peru event recorded by the SG at J9. Record length is 150 hours for Sumbawa- and 167 hours for Peru event. Note that only the spectrum from the Peru event is pressure corrected.

the minimum time series length to Fourier analyze must be larger than the time of one orbit: ∼3 hours. In order to maximize frequency resolution one has to increase the record length. In practice one faces a trade-off between frequency resolution and available signal. Increasing the time series length improves frequency resolution. However, since the modes get attenuated, there comes a point after which one adds only noise if one keeps increasing time series length. A good compromise between frequency resolution and signal-to-noise can be obtained for a record length of $1 \cdot Q$ cycles [*Dahlen*, 1979].

Earth structure is encoded in two ways in the normal mode spectra: spherically averaged Earth structure can be inferred from multiplet degenerate frequencies while aspherical structure information can be gleaned either from the splitting of individual multiplets or from the coupling between multiplets. Since the Earth is very nearly spherical one can understand that splitting and coupling of modes are subtle effects in the observed spectra and hence it should not surprise that deviations from sphericity are much less well constrained than spherically averaged earth structure.

3.1. Encoding of 1-D Earth structure in mode spectra

Estimates of multiplet degenerate frequencies can be obtained from a number of different techniques: a first set of techniques treats the effect of aspherical structure as a source of large errors and by analyzing spectra from enough earthquakes with a well distributed set of

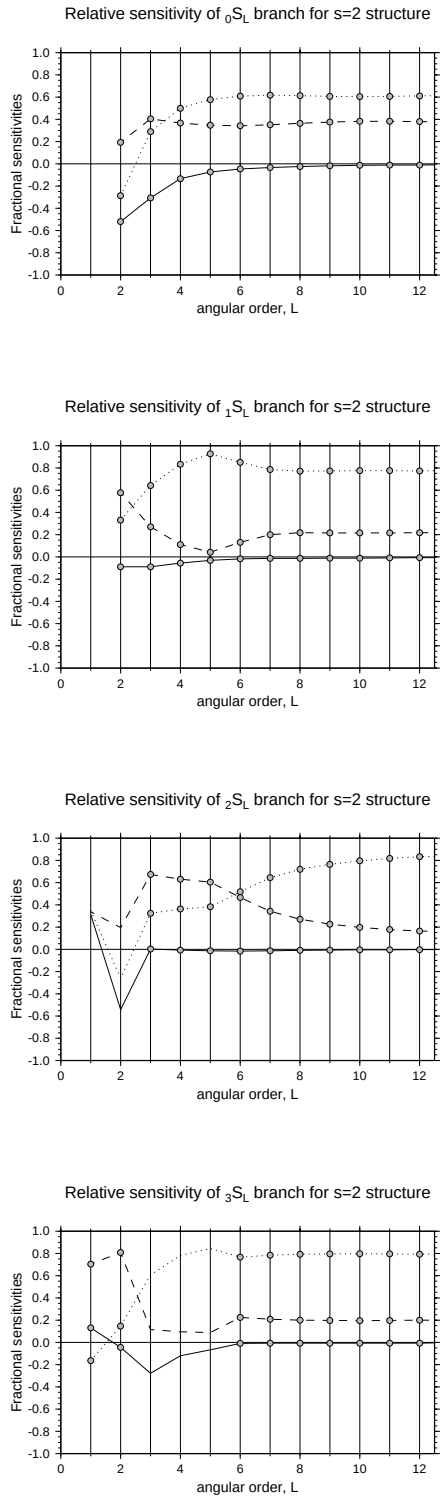

Figure 10. Relative sensitivity of aspherical structure coefficients to 3-D perturbations in Vp (dashed), Vs (dotted) and density (solid). Previously observed modes are indicated with a circular symbol. Note, that density sensitivity is only significantly different from zero for modes below 1 mHz. See also fig. 22 in *Ritzwoller and Lavely* [1995]

Table 1. Distribution of relative errors in multiplet degenerate frequency dataset used for the construction of new 1-D Earth models.

σ	$_nS_\ell$	$_nT_\ell$	$_nS_0$
1×10^{-5} – 3×10^{-5}	0	0	1
3×10^{-5} – 1×10^{-4}	56	2	13
1×10^{-4} – 3×10^{-4}	279	48	10
3×10^{-4} – 1×10^{-3}	712	198	0
1×10^{-3} – 3×10^{-3}	325	39	0

σ is the range in relative errors, $_nS_0$ are the radial modes.

stations one hopes that it will average out. (Multiplet stripping and stacking).

A second set of techniques strives to extract constraints about 3-D structure and as an aside one always also gets an degenerate frequency estimate which is largely free from bias due to effects from 3-D structure. While these techniques provide the most precise degenerate frequency estimates they can only by applied to two small subsets of modes: Histogram analysis of single record peak frequency measurements [e.g. *Smith and Masters*, 1989] while iterative spectral fitting [e.g. *Ritzwoller et al.*, 1988; *Resovsky and Ritzwoller*, 1998] and the AR method [*Masters et al.*, 2000] lend themselves only for the analysis of high-Q, low-ℓ overtones. All overtones with $\ell \geq 10$ could until recently only be analyzed with multiplet stripping. With the increasing number of high quality recordings of large earthquakes during the last decade a regionalization of the multiplet stripping technique became feasible for many high-ℓ overtones [*Widmer-Schnidrig*, 2002] which provided both improved degenerate frequency estimates as well as the first, crude 3-D constraints from these modes. Figure 7 summarizes where in the $\omega-\ell$-plane the different techniques mentioned have been applied.

The datasets used for the the analysis of high-Q, low-ℓ modes consists typically only of the ∼50 records for each of the ∼10 largest events. For the high-ℓ modes however much larger datasets are used: The regionalized multiplet stripping experiments were only possible because a dataset of 12000 individual traces (6000 vertical and 6000 horizontal component recordings) were available.

Table 1 gives the distribution of errors for a recently compiled dataset of multiplet degenerate frequencies. With this kind of dataset we are in a position to estimate all five elastic parameters (of a transversely isotropic medium) plus the density with high radial resolution

and very little trade-off between the parameters. Fig. 8 depicts the density averaging kernels obtained from the above dataset. The target uncertainty was set to 0.1 percent and the bell shaped kernels show over which depth range the model has to be integrated in order to achieve this error level. The target depth was varied from frame to frame and shows how resolution degrades with depth.

In fig. 8 the trade-off with other parameters becomes only noticeable in the core where the averaging kernels for the elastic parameters (drawn in black) are non-vanishing. This means that leakeage from elastic parameters biases the density estimates.

Since the density, ρ, is the geodynamically most interesting parameter any further improvement in the radial density profile should be welcome. The need to improve 1-D density models is emphasized by the observation, that for the discussion of the stability of stratification the relevant parameter is not the density, $\rho(r)$ but the less well resolved radial derivative $d\rho/dr$.

Here we recall two possible avenues to improve on 1-D density models: the observation of Zeeman splitting of individual multiplets and Coriolis coupling between spheroidal and toroidal multiplets. Zeeman splitting and Coriolis coupling are small signals and need to be observed with high precision before any new inference about Earth structure can be drawn from them. The reward however would be significant since these observables constitute linear constraints on the 1-D density profile much like the Earth's mass and moment of inertia. Thus, their interpretation is not subject to any trade-off with elastic parameters!

3.2. Splitting du to rotation - Zeeman splitting

The rotation of the Earth completely removes the degeneracy of a spheroidal multiplet, ${}_nS_\ell$. The frequencies of the $2\ell+1$ singlets become

$$\omega_m = \bar{\omega} + \delta\omega_m = \bar{\omega} + m\Omega\beta \quad \text{for} \quad -\ell \le m \le \ell \qquad (1)$$

with Ω the rotation rate of the Earth, $\bar{\omega}$ the multiplet degenerate frequency, and $-\ell \le m \le \ell$ the azimuthal order of the singlet and b the Zeeman splitting parameter. If the singlet frequencies of the $2\ell+1$ singlets can be observed (such as for ${}_0S_2$ in fig. 9), one can estimate b based on eq. (1). For the kth multiplet b_k is related to the distribution of density with depth through the integral relation [*Backus and Gilbert*, 1961]:

$$\beta_k = \frac{\bar{\omega}}{\Omega} b = \frac{\int \rho[2U_kV_k + V_k^2]r^2dr}{\int \rho[U_k^2 + \ell(\ell+1)V_k^2]r^2dr} \qquad (2)$$

where $U_k(r)$ and $V_k(r)$ are the usual scalar radial eigenfunction of the kth spheroidal multiplet. The denominator corresponds to the kinetic energy of the mode and is used to normalize the eigenfunctions to unity. One is thus left with a linear relation between the b_ks and the density.

Table 2. Zeeman-Splittingparameter of selected low-frequency spheroidal modes.

mode	f_{1066A}	b_{obs}	r	b_{1066A}
${}_0S_3$	0.468	4.67±0.16	3.4	4.621
${}_0S_4$	0.647	1.80±0.047	2.6	1.834
${}_0S_5$	0.840	0.83±0.028	3.4	0.840
${}_0S_6$	1.037	0.43±0.015	3.5	0.407
${}_1S_3$	0.940	2.728±0.053	1.9	2.632
${}_1S_4$	1.174	2.007±0.048	2.4	1.947
${}_1S_5$	1.371	1.489±0.067	4.5	1.436
${}_1S_8$	1.798	0.458±0.020	4.4	0.427
${}_2S_4$	1.377	0.087±0.107	122.0	0.280
${}_2S_8$	2.049	0.344±0.026	7.5	0.650
${}_2S_3$	1.241	0.612±0.082	14.0	0.667
${}_1S_2$	0.680	4.396±0.285	6.5	4.173

f is the multiplet degenerate frequency in [mHz] as predicted for model 1066A. b is the Zeeman splitting parameter in $[10^{-3}]$ from eq. (2), and r is the relative error in b in percent.

In a pilot study I estimated rotational splitting parameters (table 2) for spheroidal multiplets for which rotational splitting is expected to play a dominant role. While the errors in the splitting parameters are considerably larger than in the degenerate frequency dataset (see tab. 1), these parameters have the advantage to depend on density only and hence their interpretation is not subject to any ambiguity with the anisotropic elastic parameters.

Estimation of rotational splitting parameters is something that data from SG meters should be particularly suited for. Rotational splitting is largest for low-frequency multiplets because of their vicinity to the rotation frequency, Ω. The band below 2 mHz is also the band where the barometric pressure correction [*Zürn and Widmer*, 1995] is effective and where the best SG meters can outperform seismometers.

3.3. Coupling due to rotation: Coriolis coupling

Coriolis coupling between fundamental spheroidal and fundamental toroidal modes has been well observed between 1 and 3.5 mHz [*Masters et al.*, 1983] and more recently also in the band below 1 mHz [*Zürn et al.*, 2000]. In fact, apart from the spectra of the strain meter array at BFO [*Widmer et al.*, 1992], the SGs have contributed some of the best detections of the fundamental toroidal mode, ${}_0T_2$ which only shows up in vertical

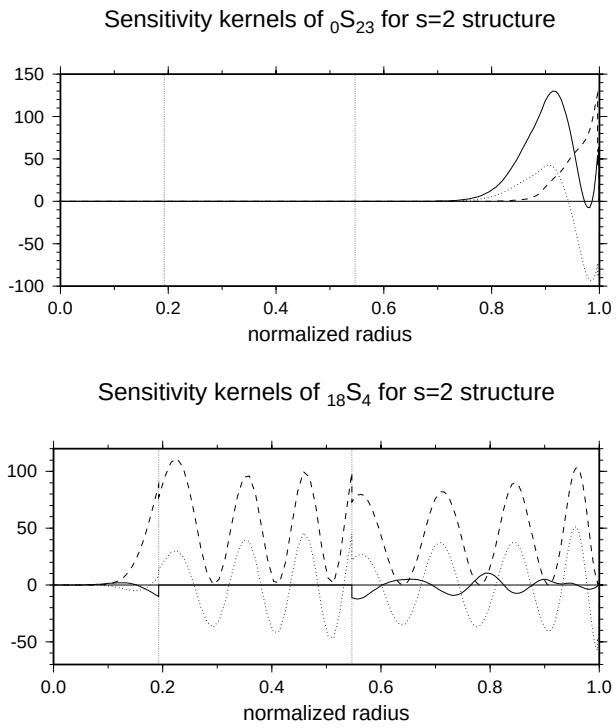

Figure 11. Sensitivity kernels for two modes with well observed structure coefficients: the fundamental mode $_0S_{23}$ and the overtone $_{18}S_4$. The Vp-kernels (dashed) and for $_0S_{23}$ also the Vs-kernel (solid) have a positive mean value while the density kernels (dotted) oscillate for both modes around a zero mean value. $_{18}S_4$ is a PKIKP-equivalent mode ans as such it is not expected to have much sensitivity to Vs structure.

component recordings through Coriolis coupling with nearby spheroidal multiplets.

Here, we only like to repeat what was already pointed out by *Zürn et al.* [2000], namely that Coriolis coupling provides linear constraints on the density profile, very similar to Zeeman splitting.

3.4. Encoding of 3-D Density structure in mode spectra

The reduced symmetry of aspherical Earth models has as a direct consequence the removal of the degeneracy of the singlet eigenfrequencies - the multiplets are split. Within the framework of first order perturbation theory this splitting can be linearly related to aspherical structure. Consider the k-th multiplet $_nS_\ell$. Its splitting can be described with the so called aspherical structure coefficients, c_s^t. The structure coefficients are linearly related to aspherical structure of harmonic degree, s, and azimuthal order, t, through [*Woodhouse and Dahlen*, 1978]:

$$ {}_kc_s^t = \int_0^a \left({}_kP_s \frac{\alpha_s^t}{\alpha_0} + {}_kS_s \frac{\beta_s^t}{\beta_0} + {}_kD_s \frac{\rho_s^t}{\rho_0} \right) dr \qquad (3) $$

where $\alpha_s^t(r)$, $\beta_s^t(r)$, $\rho_s^t(r)$ are the sought spherical harmonic expansion coefficients of Vp, Vs and density, ρ and quantities with subscript zero refer to the spherically symmetric reference model. Furthermore, $_kP_s(r)$, $_kS_s(r)$ and $_kD_s(r)$ are the kernels relating the relative volumetric perturbations of harmonic degree s to the mode splitting as represented by the aspherical structure coefficients.

The kernels of the modes $_0S_{23}$ and $_{18}S_4$ are shown in fig. 11. While Vp, Vs and density kernels are all of similar amplitude they differ in one very important aspect: Vp and Vs kernels have (at least for one of the two modes) a positive mean value while the density kernels oscillate for both modes around a zero mean. This situation is representative for all modes for which the structure coefficients, c_s^t, could be estimated. For the linear inverse problem posed in eq. 3 this means that any model with a non-zero mean for a particular spherical harmonic degree s and order t lies outside the space spanned by the set of kernels that belong to our structure coefficients! Hence our data do not allow us to make any inference on such models. To give an example: a model with a constant excess ellipticity in density of 1% ($\rho_2^0(r)/\rho_0(r) = -0.01$) leads to no additional mode splitting and cannot by reconstructed from our structure coefficients. The only exceptions are the hand full of modes below 1 mHz for which the density kernels do not integrate to zero (see fig. 10).

For completeness we mention that inversions for 3-D perturbations can also be carried out in the parameter space (μ, K, ρ). The sensitivity kernels in this representation are significantly different from the kernels in a (Vp, Vs, ρ)-representation [eq. A6 in *Ritzwoller and Lavely*, 1995]. However it turns out, that in that representation μ and ρ are well constrained model parameters while incompressibility K is as ill constrained as ρ in the (Vp, Vs, ρ)-representation. [see fig. 31 in *Ritzwoller and Lavely*, 1995].

In other words - independent of the chosen parameterization we are largely unable to estimate three independent parameters. The only exception to this bleak situation are the splittings of modes below 1 mHz which - through the effect of self-gravitation - posses additional sensitivity to density.

Whether 3-D density structure can be estimated independently of Vp and Vs structure is hotly debated in the literature. On the one hand *Ishii and Tromp* [1999] claim to succeed in the endeavor while [*Masters et al.*, 2000] present a number of inversion experiments to show that no significant improvement in the fit to the observed structure coefficients can be achieved by allowing for 3-D density structure.

The observation that density kernels in the (Vp, Vs, ρ)-representation are essentially zero mean for modes above 1 mHz constitutes a strong argument in favor of the conclusions by *Masters et al.* [2000].

4. Conclusions

We have shown, that below 1.5 mHz the most recent generation of superconducting gravimeters are competitive with the best spring gravimeters and seismometers and that for the modes below 0.6 mHz they have produced spectra with some of the highest signal-to-noise ratio sofar. The band in which SGs excel is also the band where splitting of modes possesses comparatively high sensitivity to 3-D density structure in the Earth's mantle and Core. To observe this splitting and constrain lateral density structure is one avenue of research for which SGs are uniquely suited.

Acknowledgments. I thank Walter Zürn for numerous discussions and critical inputs and Jacques Hinderer for the SG meter data from J9. The network centers of the German Regional Seismic Network, SZGRF at Erlangen and the IRIS/DMC at Seattle for archiving and distributing the data from the different sensors at BFO are greatfully acknowledged.

References

Agnew, D., and J. Berger, Vertical seismic noise at very low frequencies, *J. Geophys. Res.*, *83*, 5420–5424, 1978.

Astiz, L., and K. Creager, Noise study for the federation of digital seismic stations, *FDSN Station Book*, *1*, –, 1995.

Backus, G., and J. Gilbert, The rotational splitting of the free oscillations of the earth, *Proc. Natl. Acad. Sci.*, *47*, 362–371, 1961.

Banka, D., and D. Crossley, Noise levels of superconducting gravimeters at seismic frequencies, *Geophys. J. Int.*, *139*, 87–97, 1999.

Crossley, D., et al., Network of superconducting gravimeters benefit a number of disciplines, *EOS Trans. AGU*, *80*, 125–126, 1999.

Dahlen, F., The spectra of unresolved split normal mode multiplets, *Geophys. J. R. Astron. Soc.*, *58*, 1–33, 1979.

Ekström, G., Time domain analysis of the earth's background seismic radiation, *J. Geophys. Res.*, *106*, 26,483–26,494, 2001.

Ishii, M., and J. Tromp, Normal-mode and free air gravity constraints on lateral variations in velocity and density of the Earth's mantle, *Science*, *285*, 1231–1236, 1999.

Masters, G., J. Park, and F. Gilbert, Observations of coupled spheroidal and toroidal modes, *J. Geophys. Res.*, *88*, 10,285–10,298, 1983.

Masters, G., G. Laske, and F. Gilbert, Matrix autoregressive analysis of free-oscillation coupling and splitting, *Geophys. J. Int.*, *143*, 478–489, 2000.

Masters, T. G., and R. Widmer, Free-oscillations: frequencies and attenuations, *Global Earth Physics: A Handbook of Physical Constants*, *American Geophysical Union*, 104–125, 1995.

Nawa, K., N. Suda, Y. Fukao, T. Sato, Y. Tamura, K. Shibuya, H. McQueen, H. Virtanen, and J. Kääriäinen, Incessant excitation of the earth's free oscillations: global comparison of superconducting gravimeter records, *Phys. Earth Planet. Int.*, *120*, 289–297, 2000.

Nishida, K., N. Kobayashi, and Y. Fukao, Resonant oscillations between the solid earth and the atmosphere, *SCIENCE*, *287*, 2244–2246, 2000.

Nishida, K., N. Kobayashi, and Y. Fukao, Origin of earth's ground noise from 2 to 20 mhz, *Geophys. Res. Lett.*, *in press*, –, 2002.

Peterson, J., Observations and modeling of seismic background noise, *U. S. Geol. Surv., Open-file Rep.*, *93-322*, 1–45, 1993.

Resovsky, J., and M. Ritzwoller, New and refinded constraints on the three-dimensional earth structure from normal modes below 3 mhz, *J. Geophys. Res.*, *103*, 783–810, 1998.

Richter, B., H.-G. Wenzel, W. Zürn, and F. Klopping, From chandler wobble to free oscillations: comparison of cryogenic gravimeters and other instruments in a wide period range, *Phys. Earth Planet. Int.*, *91*, 131–148, 1995.

Ritzwoller, M., and E. Lavely, Three-dimensional seismic models of the earth's mantle, *Reviews of Geophysics*, *33*, 1–66, 1995.

Ritzwoller, M., G. Masters, and F. Gilbert, Constraining aspherical structure with low frequency interaction coefficients: Application to uncoupled multiplets, *J. Geophys. Res.*, *93*, 6369–6396, 1988.

Smith, M., and G. Masters, Aspherical structure constraints from free oscillation frequency and attenuation measurements, *J. Geophys. Res.*, *94*, 1953–1976, 1989.

Suda, N., K. Nawa, and Y. Fukao, Earth's background free oscillations, *Science*, *279*, 2089–2091, 1998.

Van Camp, M., Measuring seismic normal modes with the GWR C021 superconducting gravimeter, *Phys. Earth Planet. Inter.*, *116*, 81–92, 1999.

Warburton, R. J., and J. M. Goodkind, The influence of barometric pressure variations on gravity, *Geophys. J. R. Astron. Soc.*, *48*, 281–292, 1977.

Widmer, R., W. Zürn, and G. Masters, Observation of low order toroidal modes from the 1989 Macquarie rise event, *Geophys. J. Int.*, *111*, 226–236, 1992.

Widmer-Schnidrig, R., Application of regionalized multiplet stripping to retrieval of aspherical structure constraints, *Geophys. J. Int.*, *148*, 201–213, 2002.

Woodhouse, J., and F. Dahlen, The effect of a general aspherical perturbation on the free oscillations of the earth, *Geophys. J. R. Astron. Soc.*, *53*, 335–354, 1978.

Zürn, W., and R. Widmer, On noise reduction in vertical seismic records below 2 mHz using local barometric pressure, *Geophys. Res. Lett.*, *22*, 3537–3540, 1995.

Zürn, W., G. Laske, R. Widmer-Schnidrig, and J. Gilbert, Observation of Coriolis coupled modes below 1 mhz, *Geophys. J. Int.*, *143*, 113–118, 2000.

R. Widmer-Schnidrig, Black Forest Observatory, Institute of Geophysics, Stuttgart University, Heubach 206, D-77709 Wolfach, Germany

April 1, 2002; revised November 11, 2002; accepted December 25, 2002.